10 to 65 % [26]. Hypoalbuminemia is associated with impairment of the innate immune response; hypoalbuminemia is known to cause impairment of macrophage activation and induce macrophage apoptosis [27, 28]. Moreover, parallel to the increase in the CRP level, a decrease in the albumin level has been observed and verified in patients with various types of tumors [29, 30]. Therefore, the presence of a systemic inflammatory response, as evidenced by an elevated CRP level and hypoalbuminemia, reflects the host's immune dysfunction and should be routinely evaluated in blood chemistry examinations before surgery.

There are no studies regarding the treatment of preoperative systemic inflammation in patients with solid tumors. As mentioned above, the presence of systemic inflammation in oncology patients is closely related to the upregulation of interleukins, particularly IL-6, and impairment of the innate immune system. Identifying the mechanisms underlying the development of preoperative systemic inflammation in cancer patients could help to prevent postoperative infections. Further research is needed to determine whether preoperative systemic inflammation is a reversible phenomenon.

In summary, the results of this study indicate that a simple inflammation-based prognostic score can be used to identify patients at an increased risk of developing infectious complications following resection of gastrointestinal cancer.

Acknowledgments The following investigators assisted in this study: T. Iwnaga and T. Masuda (Kuwana City Hospital), T. Kitagawa and S. Umegae (Yokkaichi Social Insurance Hospital, Mie), T. Ikeda and H. Tonouchi (Mie Prefecture Medical Center, Mie), H. Urata and T. Fukuura (Iga Municipal Ueno General Hospital, Mie), T. Mohri and T. Kato (Toyama Hospital, Mie) and M. Ohi and J. Hiro (Mie University Hospital, Mie).

Conflict of interest No commercial sponsorship was obtained or used in the collection of data, interpretation of data or analysis of this manuscript. The authors have no conflicts of interest to declare.

References

1. Velasco E, Thuler LC, Marins CA, Dias LM, Goncalves VM. Risk factors for infectious complications after abdominal surgery for malignant disease. Am J Infect Control. 1996;24:1–6.
2. Kashimura N, Kusachi S, Konishi T, Shimizu J, Kusunoki M, Oka M, et al. Impact of surgical site infection after colorectal surgery on hospital stay and medical expenditure in Japan. Surg Today. 2012;42:639–45.
3. Tsujimoto H, Ichikura T, Ono S, Sugasawa H, Hiraki S, Sakamoto N, et al. Impact of postoperative infection on long-term survival after potentially curative resection for gastric cancer. Ann Surg Oncol. 2009;16:311–8.
4. McArdle CS, McMillan DC, Hole DJ. Impact of anastomotic leakage on long-term survival of patients undergoing curative resection for colorectal cancer. Br J Surg. 2005;92:1150–4.
5. Tang R, Chen HH, Wang YL, Changchein CR, Chen JS, Hsu KC, et al. Risk factors for surgical site infection after elective resection of the colon and rectum: a single-center prospective study of 2,809 consecutive patients. Ann Surg. 2001;234:181–9.
6. Pessaux P, Msika S, Atalla D, Hay JM, Flamant Y, French Association for Surgical Research. Risk factors for postoperative infectious complications in noncolorectal abdominal surgery. A multivariate analysis based on a prospective multicenter study of 4718 patients. Arch Surg. 2003;138:314–24.
7. Sungurtekin H, Sungurtekin U, Balci C, Zencir M, Erdem E. The influence of nutritional status on complications after major intraabdominal surgery. J Am Coll Nutr. 2004;23:227–32.
8. Sung J, Bochicchio GV, Joshi M, Bochicchio K, Costas A, Tracy K, et al. Admission serum albumin is predictive of outcome in critically ill trauma patients. Am Surg. 2004;70:1099–102.
9. Al-shaiba R, McMillan DC, Angerson WJ, Leen E, McArdle CS, Horgan P. The relationship between hypoalbuminemia, tumour volume and the systemic inflammatory response in patients with colorectal liver metastases. Br J Cancer. 2004;91:205–7.
10. Deans DA, Tan BH, Wigmore SJ, Ross JA, de Beaux AC, Paterson-Brown S, et al. The influence of systemic inflammation, dietary intake and stage of disease on rate of weight loss in patients with gastro-oesophageal cancer. Br J Cancer. 2009;100:63–9.
11. McMillan DC. An inflammation-based prognostic score and its role in the nutrition-based management of patients with cancer. Proc Nutr Soc. 2008;67:257–62.
12. McMillan DC, Crozier JE, Canna K, Angerson WJ, McArdle CS. Evaluation of an inflammation-based prognostic score (GPS) in patients undergoing resection for colon and rectal cancer. Int J Colorectal Dis. 2007;22:881–6.
13. Ishizuka M, Nagata H, Takagi K, Horie T, Kubota K. Inflammation-based prognostic score is a novel predictor of postoperative outcome in patients with colorectal cancer. Ann Surg. 2007;242:326–41.
14. Mangram AJ, Horan TC, Pearson ML, Silver LC, Jarvis WR. Guideline for prevention of surgical site infection, 1999 Centers for Disease Control and Prevention (CDC) Hospital Infection Control Practices Advisory Committee. Am J Infect Control. 1999;27(2):97–132.
15. Garner JS, Jarvis WR, Emori TG, Horan TC, Hughes JM. CDC definitions for nosocomial infections, 1988. Am J Infect Control. 1988;16:128–40.
16. Crumley AB, McMillan DC, McKernan M, McDonald AC, Stuart RC. Evaluation of an inflammation-based prognostic score in patients with inoperable gastro-oesophageal cancer. Br J Cancer. 2006;94:637–41.
17. Smyth ET, Emmerson AM. Surgical site infection surveillance. J Hosp Infect. 2000;45:173–84.
18. O'Gorman P, McMillan DC, McArdle CS. Longitudinal study of weight, appetite, performance status, and inflammation in advanced gastrointestinal cancer. Nutr Cancer. 1999;35:127–9.
19. McMillan DC, Watson WS, O'Gorman P, Preston T, Scott HR, McArdle CS. Albumin concentrations are primarily determined by the body cell mass and the systemic inflammatory response in cancer patients with weight loss. Nutr Cancer. 2001;39:210–3.
20. O'Gorman P, McMillan DC, McArdle CS. Impact of weight loss, appetite, and the inflammatory response on quality of life in gastrointestinal cancer patients. Nutr Cancer. 1998;32:76–80.
21. Moyes LH, Leitch EF, McKee RF, Anderson JH, Horgan PG, McMillan DC. Preoperative systemic inflammation predicts postoperative infectious complications in patients undergoing curative resection for colorectal cancer. Br J Cancer. 2009;100:1236–9.
22. Huang TS, Hu FC, Fan CW, et al. A simple novel model to predict mortality, surgical site infection, and pneumonia in elderly patients undergoing operation. Dig Surg. 2010;27:224–31.

23. Miki C, Konishi N, Ojima E, Hatada T, Inoue Y, Kusunoki M. C-reactive protein as a prognostic variable that reflects uncontrolled up-regulation of the IL-1-IL-6 network system in colorectal carcinoma. Dig Dis Sci. 2004;49:970–6.
24. Ikeguchi M, Hatada T, Yamamoto M, Miyake T, Matsunaga T, Fukumoto Y, et al. Serum interleukin-6 and -10 levels in patients with gastric cancer. Gastric Cancer. 2009;12:95–100.
25. Chung YC, Chang YF. Serum interleukin-6 levels reflect the disease status of colorectal cancer. J Surg Oncol. 2003;83:222–6.
26. Gibbs J, Cull W, Henderson W, Daley J, Hur K, Khuri SF. Preoperative serum albumin level as a predictor of operative mortality and morbidity: results from the National VA Surgical Risk Study. Arch Surg. 1999;134:36–42.
27. Ryan AM, Hearty A, Prichard RS, Cunningham A, Rowley SP, Reynolds JV. Association of hypoalbuminemia on the first postoperative day and complications following esophagectomy. J Gastrointest Surg. 2007;11:1355–60.
28. Reynolds JV, Redmond HP, Ueno N, Steigman C, Ziegler MM, Daly JM, et al. Impairment of macrophage activation and granuloma formation by protein deprivation in mice. Cell Immunol. 1992;139:493–504.
29. Crumley AB, Stuart RC, McKernan M, McMillan DC. Is hypoalbuminemia an independent prognostic factor in patients with gastric cancer? World J Surg. 2010;34:2393–8.
30. Fearon KC, Falconer JS, Slater C, McMillan DC, Ross JA, Preston T. Albumin synthesis rates are not decreased in hypoalbuminemic cachectic cancer patients with an ongoing acute-phase protein response. Ann Surg. 1998;227:249–54.

Am J Transl Res 2014;6(3):179-187
www.ajtr.org /ISSN:1943-8141/AJTR1401006

Review Article

In vivo optical imaging of cancer metastasis using multiphoton microscopy: a short review

Koji Tanaka[1], Yuji Toiyama[1], Yoshinaga Okugawa[1], Masato Okigami[1], Yasuhiro Inoue[1], Keiichi Uchida[1], Toshimitsu Araki[1], Yasuhiko Mohri[1], Akira Mizoguchi[2], Masato Kusunoki[1]

Departments of [1]Gastrointestinal and Pediatric Surgery, [2]Neural Regeneration and Cell Communication, Mie University Graduate School of Medicine, 2-174 Edobashi, Tsu, Mie 514-8507, Japan

Received January 7, 2014; Accepted March 10, 2014; Epub May 15, 2014; Published May 30, 2014

Abstract: Intravital (in vivo) microscopy using fluorescently-tagged proteins is a valuable tool for imaging the expression of a specific protein, its subcellular location and the dynamics of specific cell populations in living animals. Recently, multiphoton microscopy including two-photon laser scanning microscopy (TPLSM) has been used in the field of tumor biology due to its ability to image target organs at higher magnification and at deeper depths from the tissue surface for longer time periods. We developed a method of *in vivo* real-time imaging for tumor metastasis using TPLSM with an organ stabilizing system, which allow us to observe not only a single tumor cell and its microenvironment for a long time, but also to observe the same organ of the same mouse at multiple time points in preclinical models. Here, we presented *in vivo* real-time images of 1) tumor cell arrest, 2) tumor cell-platelet interaction, 3) tumor cell-leukocyte interaction, and 4) metastatic colonization at the secondary organs as representative steps of metastatic process of experimental liver metastasis models using TPLSM.

Keywords: Cancer, metastasis, multiphoton microscopy

Introduction

Cancer is a major health problem worldwide. More than 90% of cancer patients will die from metastatic disease. Therefore, translational metastasis research should be prompted urgently [1]. The underlying mechanism of tumor metastasis has being investigated using molecular biology techniques intensively. Despite of accumulating evidence of molecular biological mechanisms underlying tumor metastasis, our comprehensive understanding is still unsatisfactory [2].

Metastatic process consists of a number of steps: the detachment of tumor cells from the primary tumor mass, intravasation into blood or lymphatic vessels, escape or avoidance from the host immune system, survival in the bloodstream, arrest at the secondary distant organs, extravasation of the arrested tumor cells through vessels, and successful colonization of tumor cells in the surrounding microenvironment different from the primary tumor [3]. The underlying mechanism of each step has been examined by *in vitro* and/or *in vivo* studies.

Imaging of living animals at microscopic resolution (intravital microscopy, IVM) represents a powerful tool for understanding the dynamics of metastatic process in the natural microenvironment [4, 5]. The development of suitable mouse models is also important for intravital imaging of metastatic process.

The dorsal skinfold window chamber model remains to be used widely for IVM of invasion, intravasation, metastasis process, and tumor angiogenesis of implantable tumor [6]. This model also makes it possible to take multiple imaging sessions over several days and months. Since then, mammary window chamber model for orthotopic breast tumor [7] and cranial window chamber model for brain tumor [8] have been also developed.

Intravital imaging of metastatic process using multiphoton microscopy

Multiphoton or two-photon laser scanning microscopy (TPLSM) utilizes two-photon excitation restricted to the focal plane by high-power, pulsed lasers. The longer-wavelengths as the

two-photon excitation source can penetrate deeper into tissues, up to 1000 μm [9]. The longer-(near-infrared) wavelengths can also reduce light scattering, resulting in an increased penetration depth. The two lower-energy excitation photons cause less photodamage, or phototoxicity (photobleaching). The absence of out-of-plane fluorescence can also contribute to the reduction of phototoxicity because of the two-photon excitation only at the focal plane [9]. TPLSM offers the above-mentioned numerous imaging benefits compared with single-photon confocal laser scanning microscopy (CLSM). Thus, TPLSM is thought to be an ideal tool for intravital imaging because of its ability to keep cell viability during imaging and to allow longer imaging time.

In vivo imaging of murine liver metastasis model using TPLSM

GFP-expressing mice

Enhanced green fluorescent protein (EGFP)-transgenic C57/BL6-Tg (CAG-EGFP) mice were purchased from Japan SLC Inc. (Sizuoka, Japan). GFP-expressing nude mice (C57BL/6-BALB/c-nu/nu-EGFP) were purchased from AntiCancer Japan (Osaka, Japan).

GFP mice (20-22 g) were bred, housed in groups of six mice per cage and fed with a pelleted basal diet (CE-7, CLEA Japan Inc., Tokyo, Japan). Mice had free access to drinking water. They were kept in the animal house facilities at Mie University School of Medicine under standard conditions of humidity (50 ± 10%), temperature (23 ± 2°C) and light (12/12 h light/dark cycle), according to the Institutional Animal Care Guidelines. The experimental protocols were reviewed and approved by the Animal Care and Use Committee at Mie University Graduate School of Medicine.

RFP-expressing cancer cell line

RFP expressing murine (SL4) and human (HT-29) cancer cell lines were purchased from AntiCancer Japan (Osaka, Japan).

The inoculation of RFP-SL4 cells in GFP mice was used as a syngeneic tumor model. By contrast, the inoculation of RFP-HT29 cells in GFP nude mice was used as a xenogeneic tumor model.

Cancer cells were grown in monolayer cultures in RPMI 1640 (Sigma-Aldrich, Inc., St. Louis, MO. USA) supplemented with fetal bovine serum (FBS, 10% (v/v), GIBCO BRL, Tokyo, Japan), glutamine (2 mM), penicillin (100000 units/liter), streptomycin (100 mg/liter), and gentamycin (40 mg/liter) at 37°C in a 5% CO_2 environment. For routine passage, cultures were spilt 1:10 when they reached 90% confluence, generally every 3 days. Cells at the fifth to ninth passage were used for liver metastasis experiments, which were performed with exponential growing cells.

Murine liver metastasis model

RFP-expressing cancer cells were inoculated into the spleens of GFP mice, as a colorectal liver metastatic xenograft model [10]. RFP-HT29 or RFP-SL4 cancer cells at the fifth to ninth passage were harvested with trypsin/EDTA, and washed in serum-containing RPMI 1640 medium to inactivate any remaining trypsin. The cells were centrifuged and resuspended in phosphate-buffered saline (PBS). Finally, the cells were adjusted to 2×10^7 cells/mL for single cell suspensions.

GFP mice were anaesthetized using an anaesthetic mask with 4 L/min of isofluorane (4%; Forane, Abbott, Japan). Anaesthetic maintenance was achieved using 1.5-2% isoflurane and 4 L/min of O_2. Under direct vision, 2×10^6 cells were injected into the spleen using a 30-gauge needle through a small incision in the left lateral abdomen of anesthetized GFP mice.

Liver stabilization for *in vivo* imaging using TPLSM

Previously we have reported a method of *in vivo* real-time imaging for various murine models using TPLSM with an organ stabilizing system, which allows high magnification (×600 or higher) and high resolution (at the cellular or subcellular level) images in living animals [11-17].

Figure 1A shows an overview of liver stabilization for in vivo imaging using TPLSM. The upper midline laparotomy was made (< 15 mm) in the anaesthetized mice. The left lateral lobe of the liver was identified and exteriorized through the laparotomy (**Figure 1B**). The liver lobe was then put onto a solder lug terminal with an instant adhesive agent (KO-10-p20, DAISO, Japan)

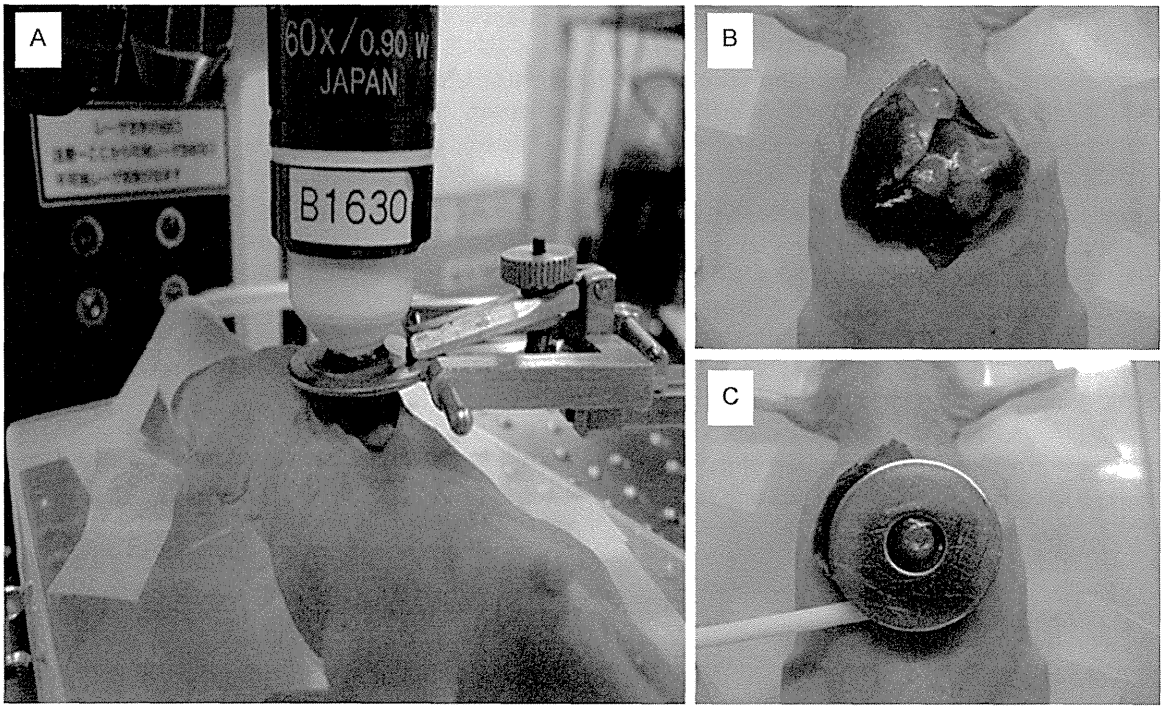

Figure 1. Overview of liver stabilization for *in vivo* imaging using TPLSM: A. Overview of liver stabilization using organ stabilizing system; B. Exteriorization of liver lobes; C. Liver stabilization using a solder lug terminal.

(**Figure 1C**). This organ stabilizer minimized the microvibration of the observed area caused by physiological heart beat and respiratory movements. After the application of PBS to the observed area, a thin cover glass was placed on the liver surface. After intravital TPLSM, a solder lug terminal was removed from the liver lobe using a release agent (KO-10-p8, DAISO, Japan). The liver surface were extensively washed by PBS to remove the residual release agent and blood coagulation mass. A sodium hyaluronate and carboxymethylcellulose membrane (Seprafilm Adhesion Barrier, Genzyme Corporation, Cambridge, MA) was placed between the liver and the abdominal wall to prevent postoperative dense adhesion. Body temperature was kept at 37°C throughout the experiments using a heating pad. Normal saline (200 μL) were administered intraperitoneally at 1-2 hour intervals for hydration during anesthesia.

TPLSM setup

The detailed procedures for TPLSM setup were described as previously [14]. In brief, experiments were performed using an upright microscope (BX61WI; Olympus, Tokyo, Japan) and a FV1000-2P laser-scanning microscope system (FLUOVIEW FV1000MPE, Olympus, Tokyo, Japan). The use of special stage risers enabled the unit to have an exceptionally wide working distance. This permitted the stereotactically immobilized, anesthetized mouse to be placed on the microscope stage. The microscope was fitted with several lenses with high numeric apertures to provide the long working distances required for *in vivo* work, and with water-immersion optics. The excitation source in TPLSM mode was Mai Tai Ti: sapphire lasers (Spectra Physics, Mountain View, CA), tuned and mode-locked at 910 nm. The Mai Tai produces light pulses of about 100 fs width (repetition rate 80 MHz). Laser light reached the sample through the microscope objectives, connected to an upright microscope (BX61WI; Olympus, Tokyo, Japan). A mean laser power at the sample was between 10 and 40 mW, depending on the depth of imaging. Microscope objective lens were 4×UPlanSApo (numerical aperture of 0.16), 10×UPlanSApo (numerical aperture of 0.4), and 60×LUMPlanFI/IR (water dipping, numerical aperture of 0.9, working distance 2 mm), respectively. Data were analyzed using a FV10-ASW (Olympus, Tokyo, Japan). TPLSM images were acquired with 512×512 pixels

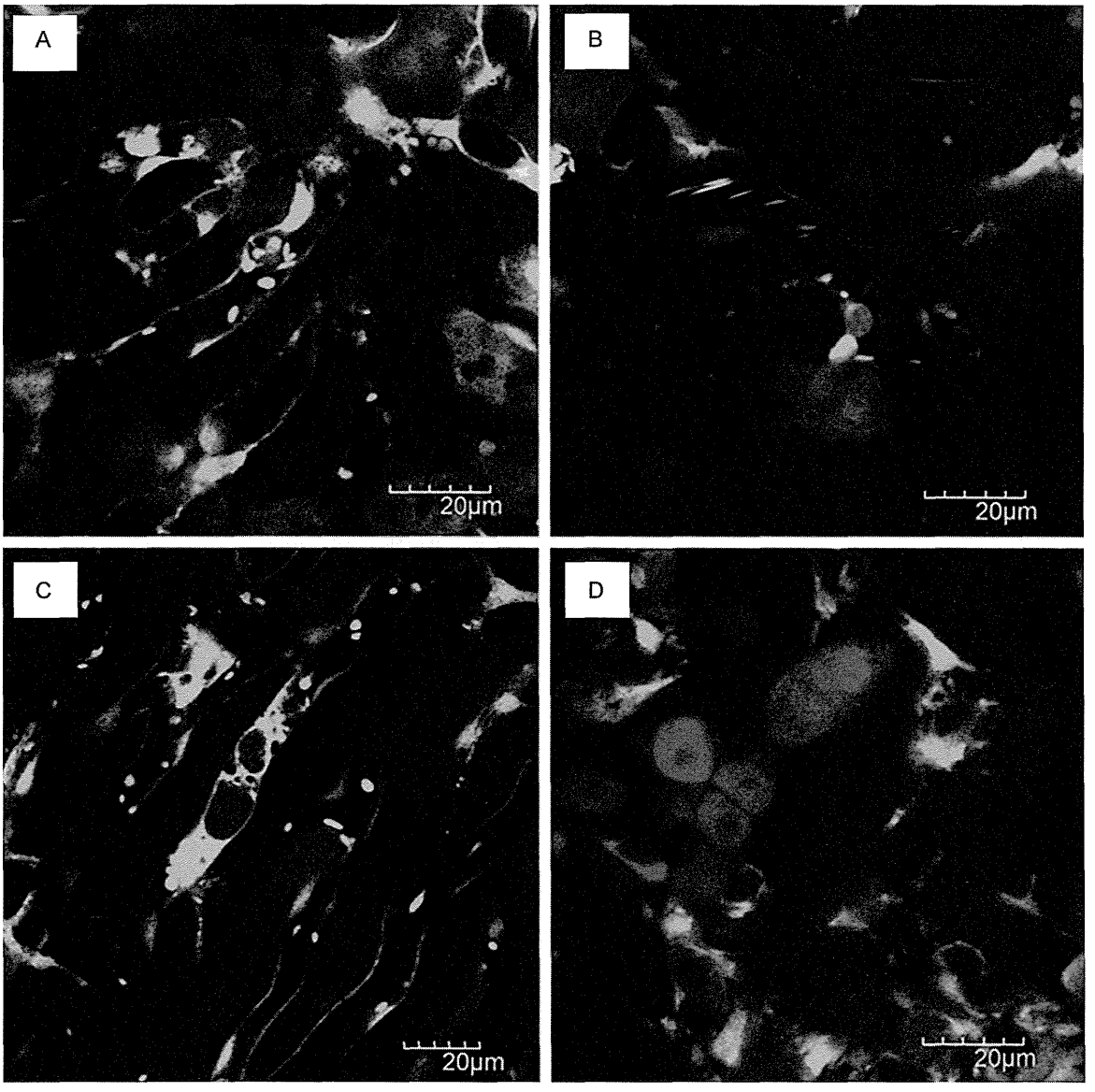

Figure 2. Visualization of liver metastatic process in xenogenic model: A. Tumor cell-platelet interaction; B. Tumor cell-leukocyte interaction; C. Platelets aggregation to the tumor cell; D. Liver metastatic colonization.

spatial resolution, from 210 μm field of view dimension, using a pixel dwelling time 4 μs. Two-photon fluorescence signals were collected by an internal detector (non-descanned detection method) at an excitation wavelength, to enable the simultaneous acquisition of EGFP signal and RFP (DsRed2) signal. Color-coded green and red images were imaged at the same time, and subsequently merged to produce single images.

Imaging methods

The surface of the liver was screened at lower magnifications by setting out the X/Y plane and adjusting the Z axis manually to detect the optimal observation area containing RFP-expressing cancer cells (at least five areas). Subsequently, each area of interest was scanned at a higher magnification (water-immersion objective 60× with or without 2× zoom) by manually setting the X/Y plane and adjusting the Z axis either automatically or manually. The scanning areas were 200×200 μm (600×) or 100×100 μm (600× with 2× zoom) respectively. The imaging depth was determined arbitrarily. The laser power was adjusted according to the imaging depth. When imaging at larger depths, we increase the laser power level (up to near 100%) manually using laser power level

controller. To image the optimal simultaneous imaging of EGFP and RFP (DsRed2), detection sensitivity (brightness by HV) was adjusted manually for EGFP (450-500) or RFP (550-600), respectively.

Visualization of liver metastatic process in xenogenic model (HT29)

Injection in the spleen or portal vein mimics hematogenous spread of tumor cells into the liver, which has been used by many researchers to create liver metastases. Tumor cells which were injected into the spleen circulated in the bloodstream (portal route), and then get stuck (or arrested) in the hepatic sinusoids. We can observe metastatic processes such as the tumor cell arrest, tumor endothelial interaction, tumor cell extravasation into the liver parenchyma, and the metastatic colonization in the liver using a liver metastasis model by intrasplenic injection of tumor cells.

Tumor cell arrest

In our study, red-colored cancer cells were visualized in the green-colored liver structures of GFP mice at the single cell level (at a magnification of over 600×). Cancer cells were arrested in hepatic sinusoids 2 hours after injection. Circulating or rolling cancer cells in hepatic vessels were never observed during the 1 hour observation time. However, cancer cells appeared to gather into the central zone of hepatic lobes. It still remains unclear whether tumor cell arrest might be caused by molecular adhesion between cancer cells and hepatic endothelial cells or size-dependent occlusion.

Tumor cell-platelet interaction

Figure 2A shows a tumor cell-platelet interaction within hepatic sinusoids. In GFP mice, red blood cells were not visualized [18]. Therefore, leukocytes were recognized as larger blood cells, and platelets were recognized as smaller ones within blood vessels. Within hepatic sinusoids, we observed that leukocytes including Kupffer cells were rolling or flowing *in vivo* real-time.

The fact that platelets are essential for hematogenous tumor metastasis has been demonstrated more than 4 decades ago and has been proven in a lot of experiments [19-21]. The interaction of tumor cells with platelets within the bloodstream occurs from the moment of tumor cell entry into the bloodstream (intravasation) to the moment that tumor cells leave from blood vessels (extravasation). Tumor cell induced platelet aggregation (TCIPA) is the phenomenon of which tumor cells can aggregate platelets. The advantageous role of TCIPA for tumor metastasis is thought to be the prolongation of tumor cell survival in the bloodstream and the protection of tumor cell by surrounding platelets from host immune system.

We observed in vivo real-time that platelets adhered to the intrasinusoidal (intravascular) tumor cells under normal blood flow, indicating a tumor cell-platelet interaction. **Figure 2C** also showed that platelets aggregated to the intrasinusoidal tumor cells like a protective coat. We think that it is thought to be a intravital imaging of TCIPA at high magnification and high resolution.

Tumor cell-leukocyte interaction

Figure 2B shows a tumor cell-leukocyte interaction. The increase in neutrophil counts or neutrophil-to-lymphocyte ratios has demonstrated to be predictive value of poor prognosis or distant metastasis in several human malignancies [22, 23]. The presence of circulating tumor cells (CTC) has been shown to be a surrogate biomarker of hematogenous metastases [24, 25]. There is increasing evidence of CTC-neutrophil interaction in vitro. The role of neutrophils in CTC recruitment to the metastatic organs has been also reported [26, 27]. The interaction between tumor cells and neutrophils is thought to play an important role in tumor metastatic cascade.

We observed that leukocytes adhered to tumor cells within hepatic sinusoids *in vivo* real-time. We previously reported an intravital imaging of a leukocyte with ameboid morphology capturing a cancer cell [14]. The leukocyte with reticular protrusions is thought to phagocytose cancer cells in hepatic sinusoids. It remains unknown whether the interaction between neutrophils and intravascular tumor cells may be related to promote metastatic colonization by enhancing tumor cell extravasation following tumor cell-endothelial interaction or to suppress tumor metastasis by phagocytosing CTCs.

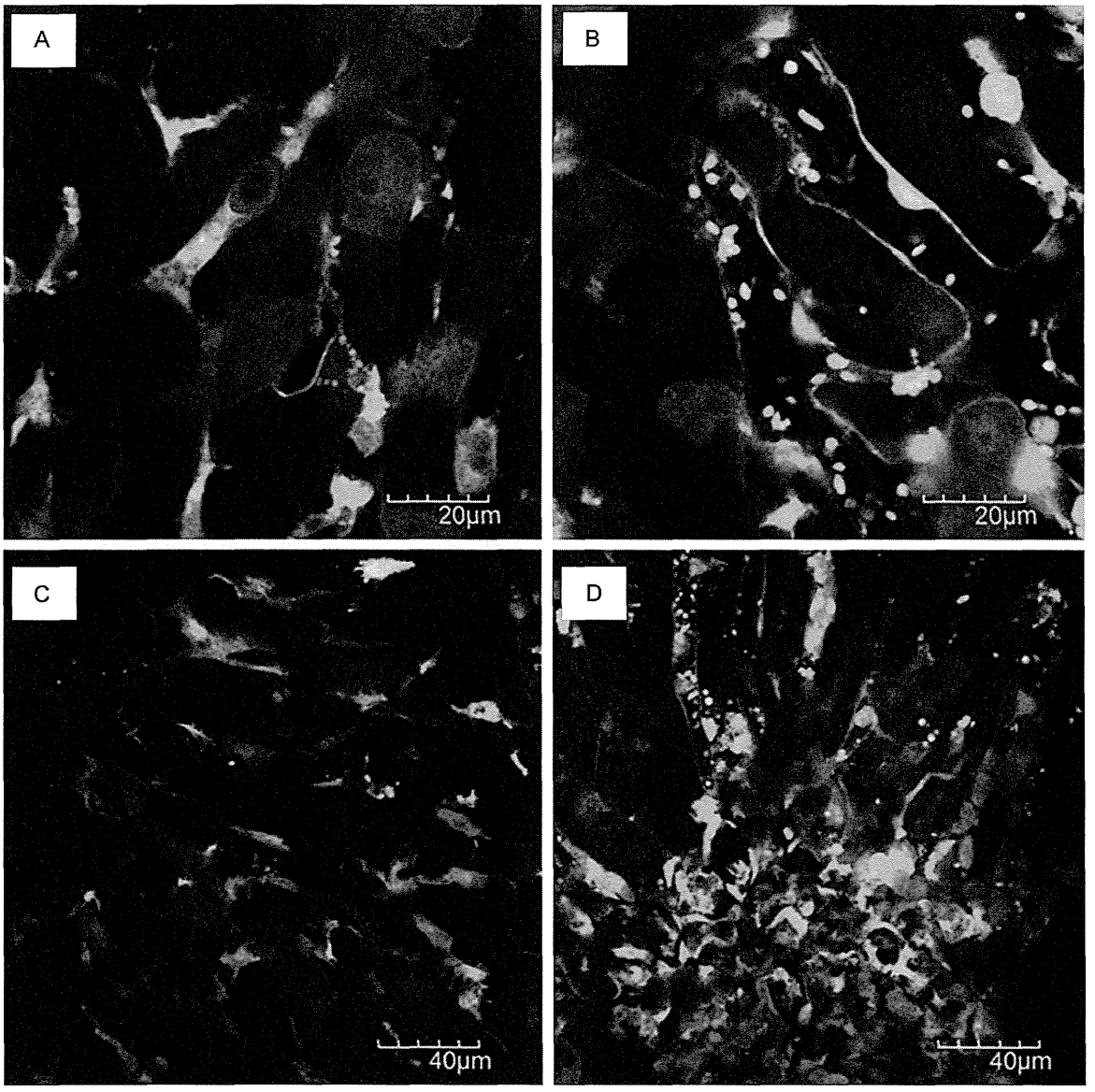

Figure 3. Visualization of liver metastatic process in syngeneic model: A. Tumor cell arrest; B. Tumor cell extravasation; C. Liver metastatic colonization showing diffuse growth pattern; D. Liver metastatic colonization with extensive stromal reaction.

Metastatic colonization at the secondary organs

It has been the challenge for long time to image *in vivo* real-time the development of micrometastases at the secondary distant organs such as liver, lung, and brain using TPLSM because of motion artifact due to cardiac and respiratory movement.

We developed a method of *in vivo* real-time TPLSM imaging for experimental metastasis models using an organ stabilizing system, which allows to observe several steps of metastatic cascade at high magnification (×600 or higher) and high resolution (at the cellular or subcellular level) in living animals [14-17].

We also developed a method of time-series (at multiple time points) intravital TPLSM imaging in the same mice over the long experimental periods by the prevention of abdominal adhesions using a sodium hyaluronate and carboxymethylcellulose membrane (Seprafilm Adhesion Barrier, Genzyme Corporation, Cambridge, MA). Time-series intravital TPLSM imaging allow to

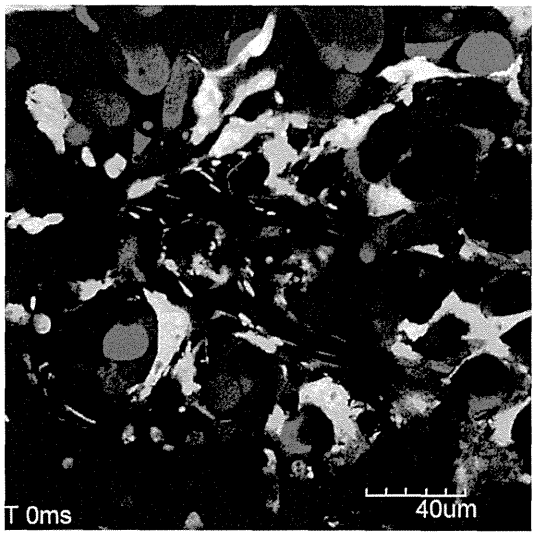

Figure 4. Tumor vessels of liver metastatic xenografts. Supplementary movie shows a time lapse imaging of a blood flow in the tumor vessels of liver metastatic xenografts.

image liver metastatic xenografts of the same mice until the formation of non-dissecting adhesions between the liver and the abdominal wall. We can take time-series images of liver metastatic xenografts in the same mice up to three time points.

Figure 2D shows a metastatic colonization of RFP-HT29 cells in the liver 2 month after the injection of tumor cells directly into the spleen. Liver metastases of RFP-HT29 showed multiple metastatic nodules macroscopically. Each metastatic nodule showed multiple micrometastatic clusters consisting of several tumor cells microscopically.

We couldn't observe the metastasis formation process continuously from a single tumor cell to micrometastatic colonization at the secondary organ because it is impossible to continue intravital TPLSM over 24 hours due to surgical stress by liver exteriorization. Therefore, it remains to be determined whether a single tumor cell retains as dormant state for long time or tumor cells directly proliferate within hepatic sinusoids (intravascular proliferation) or they proliferate in the liver parenchyma after the extravasation through hepatic endothelial cells [28].

Visualization of liver metastatic process in syngeneic model (SL4)

Tumor transplantation models of metastasis require the inoculation of human (xenograft/xenogenic) or mouse (allograft/syngeneic) cells/tissue into murine hosts. Experimental metastasis models by either xenogenic or syngenic tumor involve the injection of tumor cells directly into the vascular system, which skip the formation of a primary tumor (orthotopically or ectopically) and the invasion into the local environment. Because murine tumor cells are inoculated into the immunocompetent hosts with the same species and genetic background, syngeneic tumor models provide a valuable preclinical tool of intact tumor-host interaction by intact immune systems in the metastatic cascade.

Similar to xenogenic tumor metastasis model using RFP-HT29, tumor cell arrest (**Figure 3A**), tumor cell-platelet interaction, tumor cell-leukocyte interaction, and metastatic colonization at the secondary organs (**Figure 3C, 3D**) were observed *in vivo* real-time in syngeneic tumor metastasis model using RFP-SL4.

The space between hepatic endothelial cells and hepatocytes is named as the space of Disse (or perisinusoidal space). Spindle-shaped RFP-SL4 cells were localized in this space (**Figure 3B**). As shown in **Figure 3A**, RFP-SL4 cells are round-shaped just after intrasplenic injection. Thus, spindle-shaped RFP-SL4 cells were thought to be extravasated from hepatic sinusoids to the space of Disse 24 hours after injection.

However, we couldn't observe *in vivo* real-time the process of change in tumor cell morphology from a round-shape into a spindle-shape and the moment of intravascular tumor cells extravasate into liver parenchyma via vascular endothelium.

Figure 2D shows a metastatic colonization of RFP-HT29 cells in the liver 2 month after the injection of tumor cells directly into the spleen. Liver metastases of RFP-SL4 showed diffusely infiltrative growth macroscopically 14 days after the injection of tumor cells directly into the spleen. Microscopically, RFP-SL4 cells proliferated diffusely with extensive stromal reaction (**Figure 3C, 3D**).

Direct visualization of metastatic process at the secondary organs by TPLSM

Intravital TPLSM imaging using an organ stabilizing system can allow us to visualize each step

of metastatic cascade at high magnification and high resolution in living animals [14-17].

Time-series intravital TPLSM imaging can also allow us to visualize the same organ of the same animal at multiple time points (up to three times) during the long experimental periods. Therefore, we can directly visualize metastatic process at the secondary organs at high magnification and high resolution at least three times.

We presented *in vivo* real-time images of 1) tumor cell arrest, 2) tumor cell-platelet interaction, 3) tumor cell-leukocyte interaction, and 4) metastatic colonization at the secondary organs as representative steps of metastatic process of experimental liver metastasis models.

The spatiotemporal interactions between tumor cells and host cells during metastatic process can be visualized by using time-lapse and z-stacks imaging [14, 17]. **Figure 4** (supplementary movie 1) shows a blood flow in the tumor vessels of liver metastatic xenografts. As previously reported [15, 16], the interaction between intravascular tumor cells and endothelial cells or blood cells except for erythrocytes can be also observed. Platelet aggregation in tumor vessels and the adhesion of platelet aggregation to tumor endothelial cells were observed as the intravascular abnormalities within liver metastatic xenografts.

Although direct visualization of metastatic process at the secondary organs in vivo real-time might be valuable, there are still several issues which should be overcome. We must try to visualize the moment of each step of metastatic cascade at high magnification and high resolution in living animals. In our procedure, we couldn't observe the metastasis formation process continuously from a single tumor cell to micrometastatic colonization. We couldn't also observe the moment of change in tumor cell morphology or the moment of metastatic colonization by tumor cell division.

Direct visualization of metastatic process by real-time imaging for extended periods (over 24 hours per session) will help us to understand the spatiotemporal tumor-host interaction on tumor metastasis at the cellular and subcellular levels.

Disclosure of conflict of interest

None.

Address correspondence to: Koji Tanaka, Department of Gastrointestinal and Pediatric Surgery, Mie University Graduate School of Medicine, 2-174 Edobashi, Tsu, Mie 514-8507, Japan. Tel: 81-59-231-5294; Fax: 81-59-232-6968; E-mail: qouji@clin.medic.mie-u.ac.jp

References

[1] Sleeman J, Steeg PS. Cancer metastasis as a therapeutic target. Eur J Cancer 2010; 46: 1177-80.

[2] Valastyan S, Weinberg RA. Tumor metastasis: molecular insights and evolving paradigms. Cell 2011; 147: 275-92.

[3] Mathot L, Stenninger J. Behavior of seeds and soil in the mechanism of metastasis: a deeper understanding. Cancer Sci 2012; 103: 626-31.

[4] Pittet MJ, Weissleder R. Intravital imaging. Cell 2011; 147: 983-91.

[5] Beerling E, Ritsma L, Vrisekoop N, Derksen PW, van Rheenen J. Intravital microscopy: new insights into metastasis of tumors. J Cell Sci 2011; 124: 299-310.

[6] Hak S, Reitan NK, Haraldseth O, de Lange Davies C. Intravital microscopy in window chambers: a unique tool to study tumor angiogenesis and delivery of nanoparticles. Angiogenesis 2010; 13: 113-30.

[7] Kedrin D, Gligorijevic B, Wyckoff J, Verkhusha VV, Condeelis J, Segall JE, van Rheenen J. Intravital imaging of metastatic behavior through a mammary imaging window. Nat Methods 2008; 5: 1019-21.

[8] Kienast Y, von Baumgarten L, Fuhrmann M, Klinkert WE, Goldbrunner R, Herms J, Winkler F. Real-time imaging reveals the single steps of brain metastasis formation. Nat Med 2010; 16: 116-22.

[9] Ustione A, Piston DW. A simple introduction to multiphoton microscopy. J Microsc 2011; 243: 221-6.

[10] de Jong GM, Aarts F, Hendriks T, Boerman OC, Bleichrodt RP. Animal models for liver metastases of colorectal cancer: research review of preclinical studies in rodents. J Surg Res 2009; 154: 167-76.

[11] Toiyama Y, Mizoguchi A, Okugawa Y, Koike Y, Morimoto Y, Araki T, Uchida K, Tanaka K, Nakashima H, Hibi M, Kimura K, Inoue Y, Miki C, Kusunoki M. Intravital imaging of DSS-induced cecal mucosal damage in GFP-transgenic mice using two-photon microscopy. J Gastroenterol 2010; 45: 544-53.

[12] Koike Y, Tanaka K, Okugawa Y, Morimoto Y, Toiyama Y, Uchida K, Miki C, Mizoguchi A, Kusunoki M. In vivo real-time two-photon microscopic imaging of platelet aggregation induced by selective laser irradiation to the endothelium created in the beta-actin-green fluorescent protein transgenic mice. J Thromb Thrombolysis 2011; 32: 138-45.
[13] Morimoto Y, Tanaka K, Toiyama Y, Inoue Y, Araki T, Uchida K, Kimura K, Mizoguchi A, Kusunoki M. Intravital three-dimensional dynamic pathology of experimental colitis in living mice using two-photon laser scanning microscopy. J Gastrointest Surg 2011; 15: 1842-50.
[14] Tanaka K, Morimoto Y, Toiyama Y, Okugawa Y, Inoue Y, Uchida K, Kimura K, Mizoguchi A, Kusunoki M. Intravital dual-colored visualization of colorectal liver metastasis in living mice using two photon laser scanning microscopy. Microsc Res Tech 2012; 75: 307-15.
[15] Tanaka K, Morimoto Y, Toiyama Y, Matsushita K, Kawamura M, Koike Y, Okugawa Y, Inoue Y, Uchida K, Araki T, Mizoguchi A, Kusunoki M. In vivo time-course imaging of tumor angiogenesis in colorectal liver metastases in the same living mice using two-photon laser scanning microscopy. J Oncol 2012; 2012: 265487.
[16] Tanaka K, Okigami M, Toiyama Y, Morimoto Y, Matsushita K, Kawamura M, Hashimoto K, Saigusa S, Okugawa Y, Inoue Y, Uchida K, Araki T, Mohri Y, Mizoguchi A, Kusunoki M. In vivo real-time imaging of chemotherapy response on the liver metastatic tumor microenvironment using multiphoton microscopy. Oncol Rep 2012; 28: 1822-30.
[17] Tanaka K, Toiyama Y, Inoue Y, Uchida K, Araki T, Mohri Y, Mizoguchi A, Kusunoki M. Intravital imaging of gastrointestinal diseases in preclinical models using two-photon laser scanning microscopy. Surg Today 2013; 43: 123-9.
[18] Okabe M, Ikawa M, Kominami K, Nakanishi T, Nishimune Y. 'Green mice' as a source of ubiquitous green cells. FEBS Lett 1997; 407: 313-9
[19] Erpenbeck L, Schön MP. Deadly allies: the fatal interplay between platelets and metastasizing cancer cells. Blood 2010; 115: 3427-36.
[20] Gay LJ, Felding-Habermann B. Contribution of platelets to tumour metastasis. Nat Rev Cancer 2011; 11: 123-34.
[21] Buergy D, Wenz F, Groden C, Brockmann MA. Tumor-platelet interaction in solid tumors. Int J Cancer 2012; 130: 2747-60.
[22] Ubukata H, Motohashi G, Tabuchi T, Nagata H, Konishi S, Tabuchi T. Evaluations of interferon-γ/interleukin-4 ratio and neutrophil/lymphocyte ratio as prognostic indicators in gastric cancer patients. J Surg Oncol 2010; 102: 742-7.
[23] Liu H, Liu G, Bao Q, Sun W, Bao H, Bi L, Wen W, Liu Y, Wang Z, Yin X, Bai Y, Hu X. The baseline ratio of neutrophils to lymphocytes is associated with patient prognosis in rectal carcinoma. J Gastrointest Cancer 2010; 41: 116-20.
[24] Yu M, Stott S, Toner M, Maheswaran S, Haber DA. Circulating tumor cells: approaches to isolation and characterization. J Cell Biol 2011; 192: 373-82.
[25] Ghadially R. The role of stem and circulating cells in cancer metastasis. J Surg Oncol 2011; 103: 555-7.
[26] Huh SJ, Liang S, Sharma A, Dong C, Robertson GP. Transiently entrapped circulating tumor cells interact with neutrophils to facilitate lung metastasis development. Cancer Res 2010; 70: 6071-82.
[27] Spicer JD, McDonald B, Cools-Lartigue JJ, Chow SC, Giannias B, Kubes P, Ferri LE. Neutrophils promote liver metastasis via Mac-1-mediated interactions with circulating tumor cells. Cancer Res 2012; 72: 3919-27.
[28] Robertson JH, Sarkar S, Yang SY, Seifalian AM, Winslet MC. In vivo models for early development of colorectal liver metastasis. Int J Exp Pathol 2008; 89: 1-12.

Surg Today (2013) 43:1095–1102
DOI 10.1007/s00595-013-0504-x

ORIGINAL ARTICLE

Factors influencing the outcome of image-guided percutaneous drainage of intra-abdominal abscess after gastrointestinal surgery

Yoshiki Okita · Yasuhiko Mohri · Minako Kobayashi · Toshimitsu Araki · Koji Tanaka · Yasuhiro Inoue · Keiichi Uchida · Koichiro Yamakado · Kan Takeda · Masato Kusunoki

Received: 16 February 2012 / Accepted: 19 July 2012 / Published online: 14 February 2013

Abstract
Purpose To improve the selection of patients for percutaneous abscess drainage (PAD) to treat postoperative intra-abdominal abscess after gastrointestinal surgery, we investigated the factors predictive of outcome.
Methods Of 143 consecutive patients with symptomatic postoperative intra-abdominal abscess after a gastrointestinal tract resection, 104 who underwent image-guided PAD as the initial treatment were reviewed. We assessed the possible associations between successful PAD and patient-, abscess-, surgical-, and drainage-related variables, and investigated the success rates of PAD for patients with vs. those without the factors related to successful outcome.
Results Based on monitoring for 1 year after PAD, the success rate of this procedure was 85.6 % (89/104). Multivariate analysis revealed that the interval between surgery and the onset of abscess ($p = 0.0234$) and a single abscess ($p = 0.0038$) were independently associated with a successful outcome. Single late-onset abscess resolved completely within 10 weeks in 91.4 % of these patients.
Conclusions Despite new strategies aimed at preventing surgical site infection, PAD remains an important factor in the postoperative management of gastrointestinal surgery in Japan. Initial recognition of the day of onset and the number of abscesses are important prognostic factors.

Y. Okita (✉) · Y. Mohri · M. Kobayashi · T. Araki · K. Tanaka · Y. Inoue · K. Uchida · M. Kusunoki
Departments of Gastrointestinal and Pediatric Surgery, Mie University Graduate School of Medicine, 2-174 Edobashi, Tsu, Mie 514-8507, Japan
e-mail: nyokkin@clin.medic.mie-u.ac.jp

K. Yamakado · K. Takeda
Department of Radiology, Mie University Graduate School of Medicine, 2-174 Edobashi, Tsu, Mie 514-8507, Japan

Keywords Postoperative intra-abdominal abscess · Percutaneous abscess drainage · CT-guided drainage

Introduction

Intra-abdominal abscess is a frequent cause of morbidity and mortality following surgery of the alimentary tract [1, 2]. In the past three decades, advances in image-guided percutaneous abscess drainage (PAD) have provided a safe and effective alternative to surgical drainage [3–7]. Despite the lack of randomized studies comparing percutaneous to surgical drainage, PAD has become a widely accepted treatment for accessible postoperative intra-abdominal abscess, especially in Western countries [8–12]. However, the concepts of treatment for postoperative intra-abdominal abscess after gastrointestinal surgery differ between Japan and Western countries [13]. In Japan, routine abdominal drains are generally placed to facilitate the diagnosis of anastomotic leakage and reduce the risk of intra-abdominal abscess formation [14, 15], although increasing evidence suggests that prophylactic drains do not reduce the incidence of postoperative complications following a variety of intra-abdominal procedures [16]. Routine abdominal drains also play a therapeutic role when intra-abdominal abscess develops after surgery [13]. However, with the increasing use of CT-guided drainage, the indications for PAD have expanded.

The current study focuses on how patient-, surgery-, abscess- and drainage-related factors affect the outcome of PAD, since the implementation of standard surgical site infection prevention policies in Japan. We investigated the effectiveness and safety of PAD, and identified the factors predictive of its successful outcome, to improve the selection of patients who would benefit from this procedure

for postoperative intra-abdominal abscess following gastrointestinal surgery.

Methods

Patients

Our surgical site infection database identified 143 patients with a symptomatic postoperative intra-abdominal abscess diagnosed after gastrointestinal surgery, between January 2002 and March 2010, at Mie University Hospital. Among these, 104 patients received image-guided PAD as the initial treatment. The 39 patients who did not receive image-guided PAD initially were treated with open surgical drainage ($n = 16$), antibiotic therapy alone ($n = 16$), or transanal drainage ($n = 7$). The study group included 71 men and 33 women, with a mean age of 51 ± 2 years (mean ± SE, range 14–91). The primary diseases and initial surgical procedures are summarized in Tables 1 and 2, respectively. Gastrointestinal surgery was performed for malignant disease in 47 (45.2 %) patients and for inflammatory bowel disease in 41 (39.4 %) patients. Asymptomatic radiographical enteric fistulae without abscess were not included. Intra-abdominal abscess was suspected with the development of such symptoms as abdominal pain, pyrexia, leucocytosis, and shock. The abscess was diagnosed by CT scan in all cases and defined as an infected fluid collection identified by image-guided needle aspiration during image-guided PAD. Recurrent abscess after restorative surgery for previous postoperative intra-abdominal abscess was excluded, so that patients were not included more than once. When severe diffuse peritonitis or septic shock was suspected, open surgical drainage was performed. Patients with an abscess that could not be treated by PAD, in the absence of signs of peritonitis, were treated with antibiotic therapy alone. Transanal drainage was performed for enteric fistula just above the anus, caused by anastomotic leakage after surgery such as low anterior resection, and when PAD carried a risk of injury to other abdominal organs or major vessels.

Table 1 Underlying primary disease

	n
Colorectal cancer	28
Ulcerative colitis	24
Gastric cancer	19
Crohn's disease	17
Colon diverticula	4
Acute appendicitis	4
Adhesive small bowel obstruction	3
Others	5

Table 2 Initial surgical procedures

	n
Gastric surgery	
Total gastrectomy	10
Distal gastrectomy	8
Small intestinal surgery	
Small bowel resection	11
Ileostomy closure	11
Stoma construction	6
Ileoanal reanastomosis	3
Appendectomy	4
Colorectal surgery	
Rectal resection	13
Right hemicolectomy	9
Restorative proctocolectomy with ileal pouch anal anastomosis	9
Subtotal colectomy with ileorectal anastomosis	4
Left hemicolectomy	4
Subtotal colectomy without ileorectal anastomosis	3
Transverse colon resection	3
Sigmoidectomy	2
Ileocolorectal or colorectal anastomosis after Hartman's procedure	2
Abdominal perineal resection	1
Colostomy closure	1

Indications and procedure for PAD to treat postoperative intra-abdominal abscess

PAD was attempted as the initial procedure only if an abscess could be accessed without risk of injury to other abdominal organs, if severe diffuse peritonitis was not suspected, and in the absence of septic shock at presentation, based on judgment of the surgeon and interventional radiologist. All procedures were performed under local anesthesia and image guidance: as CT-guided PAD in 83 patients and as ultrasound-guided PAD in 21 patients. The attending interventional radiologist decided on the size and number of catheters used, based on the nature of the fluid obtained at needle aspiration and the extent of the abscess. The catheter size ranged from 8 to 12 F and Pigtail drainage catheters (Skater Drainage Catheter; Angiotech, Stenlose, Denmark) were placed in the abscess cavity using the Trocar method or Seldinger technique. When abscess drainage was insufficient, the catheter was replaced by a thicker one, inserted using an over-the-guidewire technique or it was moved to a position that allowed sufficient drainage. Bags were attached for gravity drainage after placing a stopcock at the external end of the catheter for routine irrigation. Abscess cavities of all patients who

underwent PAD were irrigated with natural saline from drainage tubes about 1 week after PAD. No concomitant antibiotics were given before puncture of the PAD and/or during PAD when the abscesses were localized with mild symptoms, based on the judgment of the surgeon. However, concomitant antibiotics were administered to patients with severe symptoms. Antibiotics were initially chosen empirically and changed, if necessary, based on culture and sensitivity results.

Definition of outcomes

Patients were divided into two groups depending on whether the PAD outcome was successful. Success was defined as complete resolution of the intra-abdominal abscess or enteric fistula after one or more PAD procedures without the need for surgery. Complete resolution of the intra-abdominal abscess was defined as radiological disappearance of the abscess cavity and clinical disappearance of the symptoms. The catheter was removed after CT or fluoroscopy confirmed complete resolution of the fluid collection or enteric fistula. When recurrent intra-abdominal abscesses had been drained and resolved completely, the outcome of PAD was defined as successful. The "success group" did not include any patients in whom PAD was subsequently deemed to have failed in the follow-up period. Failure was defined as the need for elective interval surgery or emergency surgery after PAD. Patients with a postoperative intra-abdominal abscess were monitored for at least 1 year after PAD and their outcomes were judged according to the definitions of success and failure.

Definition of variables

The potential success factors were as follows

Patient-related factors age at surgery, gender, malignant disease, inflammatory bowel disease, steroid treatment, diabetes mellitus, and laboratory data just before PAD (white blood cell count, hemoglobin, CRP, ALB, choline esterase).

Surgery-related factors surgical procedure, stoma construction, anastomotic operation, surgical duration, operative blood loss, and wound class.

Abscess-related factors interval between surgery and onset, interval between onset and PAD, size and number of abscess/es.

Drainage-related factors drainage procedure, concomitant use of antibiotic therapy, duration of antibiotic therapy, multiple drains, and need for additional PAD.

The surgical procedure and wound class were categorized according to the National Nosocomial Infections Surveillance System. Surgical procedures were divided into gastric surgery (GAST), small bowel surgery (SB), appendectomy (APPY), and colorectal surgery (COLO). The wound class comprised four criteria: clean, clean-contaminated, contaminated, or dirty [17]. The day of onset was defined as the day when patients complained of symptoms related to the abscess. Common presenting symptoms included pyrexia, abdominal tenderness, and abdominal fullness.

Abscess location on CT scans was categorized into nine areas: right subphrenic, Subhepatic/Morson's pouch, right gutter, left subphrenic/perisplenic, left gutter, peripancreas/lesser sac, pelvis/perirectal, below the abdominal wall, and other interperitoneal. A single abscess was defined as an abscess found in a single location, whereas multiple abscesses were defined as abscesses located in more than two locations. Duration in the cumulative success rate of PAD was defined as the interval between PAD puncture and complete resolution of the abscess.

Statistical analysis

Quantitative data are expressed as mean ± SE (range). Comparisons between the success group and the failure group were analyzed by the Chi-square test with Yate's correction and the Mann–Whitney U test for quantitative and qualitative variables, using Statview 4.5 software (Abacus Concepts, Berkeley, CA, USA). Univariate analysis was used to examine the relationship between the success of PAD and the variables studied. All variables associated with the failure group resulting in $p < 0.1$ on univariate analysis were examined consecutively by multivariate analysis logistic regression. A p value of <0.05 was considered significant. Correlation between the enteric fistulae and a single or late-onset abscess was analyzed by the Chi-square test with Yate's correction.

Results

Outcome after PAD for postoperative intra-abdominal abscess

The success rate of PAD at 1 year was 85.6 % ($n = 89$), although 24 of these patients required repeat drainage. The failure group consisted of six patients who underwent emergency operations for peritonitis, and nine patients who underwent or needed to undergo elective operations for enteric fistulae. Table 3 summarizes the clinical characteristics and outcomes of these 15 patients. Six patients required emergency conversion to open surgical drainage and stoma construction after PAD because of peritonitis originating from enteric fistulae. In eight patients, the enteric fistulae were not closed and elective surgery was

Table 3 Clinical characteristics and outcome of the 15 patients in the failure group

Case	Age	Gender	Types of primary disease	Procedure of restorative operation	Emergency/ Elective	Intervals between initial PAD and restorative operation
1	19	M	UC	Open surgical drainage and stoma construction	Emergency	1
2	22	M	UC	Open surgical drainage and stoma construction	Emergency	1
3	25	F	UC	Open surgical drainage and stoma construction	Emergency	1
4	75	F	Colorectal cancer	Open surgical drainage and stoma construction	Emergency	2
5	91	M	Adhesive small bowel obstruction	Open surgical drainage and stoma construction	Emergency	2
6	79	M	Colorectal cancer	Open surgical drainage and stoma construction	Emergency	5
7	64	M	Colorectal cancer	Reanastomosis without stoma construction	Elective	32
8	30	M	CD	Stoma construction	Elective	57
9	32	M	CD	Reanastomosis with dysfunctional stoma construction	Elective	74
10	38	M	Gastric cancer	gastro-jejunal bypass	Elective	88
11	34	M	CD	Stoma construction	Elective	148
12	25	M	UC	Stoma construction	Elective	171
13	15	F	CD	Reanastomosis without stoma construction	Elective	364
14	37	F	CD	Reanastomosis without stoma construction	Elective	720
15[a]	71	F	Colorectal cancer	–	–	–

UC ulcerative colitis, *CD* Crohn's disease, *PAD* percutaneous abscess drainage

[a] Patients with persistent enteric fistulae for over 1 year

needed later. All enteric fistulae during PAD were confirmed by fluoroscopy. In one patient, the enteric fistula persisted for over 1 year and elective surgery was scheduled. All of the 'failure group' patients had enteric fistulae. No patient died after PAD in this series. There was one major complication related to PAD; namely, massive bleeding from long-term placement, in a patient from the success group.

Factors associated with successful outcome

Univariate analysis showed that a higher white blood cell count tended to be associated with successful PAD, but there were no other differences in patient- and surgery-related factors between the success and failure groups (Table 4). A longer interval between surgery and onset and having a single abscess were also associated with success, but there were no other differences in abscess- and drainage-related factors between the success and failure groups (Table 5). Multivariate analysis was performed using three variables (Table 6): white blood cell count, interval between surgery and onset, and single abscess. Multivariate analysis showed that a longer interval between surgery and onset (odds ratio = 1.248; 95 % CI 1.031–1.510; $p = 0.0232$) and having a single abscess (odds ratio = 7.690; 95 % CI 1.899–31.136; $p = 0.0042$) were significantly associated with the successful outcome of PAD.

Success rates of PAD for patients with vs. those without factors related to outcome

The median interval between surgery and the onset of intra-abdominal abscess was 8 days, the onset being early (<8 days) in 55 patients and late (>9 days) in 49 patients. Patients were divided into two groups according to the presence or absence of factors related to a successful outcome. Group A ($n = 35$) comprised patients with a single and late-onset abscesses and group B ($n = 69$) comprised patients with multiple and/or early onset abscesses. Figure 1 shows the cumulative success rates of PAD in Groups A and B. The success rate of PAD in Group A was 97.1 % (34/35), with a median PAD period of 14 days and

Table 4 Patient-related and surgery-related factors divided into success and failure groups

Factors	Success group ($n = 89$)	Failure group ($n = 15$)	p value
Age at surgery (years)	52 ± 2	44 ± 6	0.2116
Gender (M/F)	61/28	10/5	>0.9999
Malignant disease (Y/N)	44/45	6/9	0.6910
Inflammatory bowel disease (Y/N)	32/57	9/6	0.1396
Preoperative intra-abdominal abscess(Y/N)	7/82	3/12	0.1403
Steroid treatment (Y/N)	22/67	4/11	>0.9999
Diabetes mellitus (Y/N)	8/88	0/15	0.5987
White blood cell count (/mm^3)	12400 ± 500	11800 ± 2400	0.0663
Hemoglobin (g/dl)	10.0 ± 0.2	10.4 ± 0.5	0.6206
CRP (mg/d)	12.6 ± 0.8	15.0 ± 2.3	0.3548
ALB (g/dl)	3.0 ± 0.1	2.9 ± 0.1	0.3222
Choline esterase (ΔpH)	0.48 ± 0.02	0.50 ± 0.06	0.8464
Categories of surgical procedure (GAST/SB/APPY/COLO)	17/25/4/43	1/7/0/7	0.3521
Stoma construction (Y/N)	34/55	2/13	0.1142
Anastomotic operation (Y/N)	73/16	12/3	>0.9999
Surgical duration (min)	272 ± 13	227 ± 27	0.1612
Operative blood loss (g)	523 ± 53	360 ± 110	0.3920
Wound class (CC/CO/D)	66/13/10	10/4/1	0.4738

GAST gastric surgery, *SB* small bowel surgery, *APPY* appendectomy, *COLO* colorectal surgery, *CC* clean-contaminated operation, *CO* contaminated operation, *D* dirty/infected operation

Table 5 Abscess- and drainage-related factors divided into "success" and "failure" groups

Factors	Success group ($n = 89$)	Failure group ($n = 15$)	p value
Interval between surgery and onset (days)	10 ± 1	6 ± 1	0.0003
Interval between onset and PAD (days)	3 ± 0	4 ± 2	0.1679
Size of abscess (<5 cm)	23/66	2/13	0.4701
Single abscess (Y/N)	63/26	3/12	0.0005
Drainage procedure (CT/US)	73/16	10/5	0.9434
Concomitant use of antibiotics therapy (Y/N)	69/16	4/2	0.3064
Duration of antibiotics therapy (days)	8 ± 1	7 ± 2	0.9268
Multiple drain (Y/N)	24/65	6/9	0.4699
Number of drainage tube	1.5 ± 0.1	1.6 ± 0.2	0.4762
Additional PAD (Y/N)	19/70	5/10	0.4915

PAD percutaneous abscess drainage

complete resolution within 10 weeks (70 days) in 91.4 % (32/35) and sometime after 10 weeks in 5.7 % (2/35). The success rate of PAD in Group B was 79.7 % (55/69), with a median PAD period of 21 days and complete resolution within 10 weeks in 76.8 % (53/69) and sometime after 10 weeks in 2.9 % (2/69).

Table 6 Logistic regression analysis for factors associated with successful outcome

	Odds ratio	95 % CI	p value
White blood cell count (/mm^3)	1.038	0.916–1.175	0.5605
Interval between surgery and onset (days)	1.248	1.031–1.510	0.0232
Single abscess (Y/N)	7.690	1.899–31.136	0.0042

Association between the absence of enteric fistulae and a single and late-onset abscess

All enteric fistulae were confirmed during PAD by fluoroscopy and detected in 53 patients (51.0 %). No significant correlation was found between the absence of enteric fistulae and a single and late-onset abscesses ($p = 0.1660$).

Success rate of PAD for patients with abscess related to an enteric fistula

The success rate of PAD among patients with an abscess related to enteric fistulae was 71.7 % with no difference in outcome between small intestinal fistulae and large intestinal fistulae ($p = 0.8036$). Factor XIII concentrate was injected during drainage for five patients with an enteric fistula, resulting in success in four. The success rate of PAD was 92.9 % (13/14) for patients with a single and late-onset abscess related to enteric fistulae but only

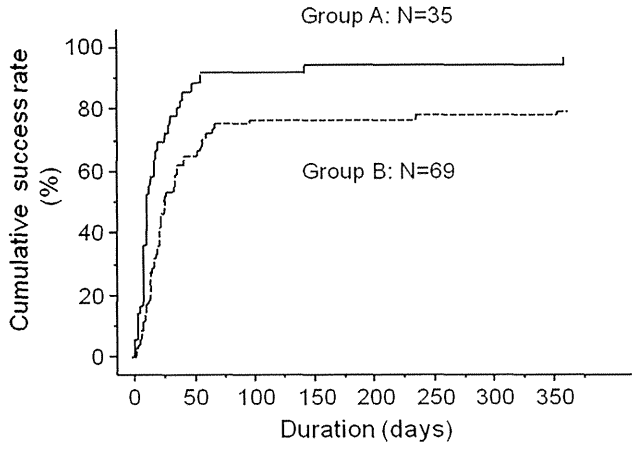

Fig. 1 The cumulative success rate of percutaneous abscess drainage in 104 patients increased with therapeutic duration. The success rate was 85.6 % ($n = 89$) after 1 year of follow-up

64.1 % (25/39) for patients with multiple and/or early onset-abscesses related to enteric fistulae.

Discussion

PAD was first described in the late 1970s and in 1981; Gerzof et al. [3] reported a success rate of 86 % when used to treat intra-abdominal abscesses in 67 patients. Subsequently, it was demonstrated that the effectiveness and safety of PAD [8, 18–20], which over the last 30 years, made the transition from a revolutionary to a routine procedure, replacing open surgical drainage, except in the most difficult or inaccessible cases. Using univariate analysis, several authors have identified the factors predictive of the failure of PAD, including enteric fistulae, multiple or loculated abscesses, large abscesses, necrotic tissue, and pancreatic localization [3, 8, 11, 21–24].

Percutaneous drainage has been used in the management of complex abscesses, including multiple abscesses, those associated with fistulae, splenic abscesses, and infected fluid collections whose drainage route traversed normal organs) [7]. The use of PAD for patients with complex abscesses has been suggested to offer significant therapeutic benefits, even though it may not be curative and surgery could still be required [4, 25]. A study of the literature revealed a success rate of 45–88 % for PAD treating complex abscesses [20, 26–28].

Some postoperative intra-abdominal abscesses associated with anastomotic leaks lead to diffuse peritonitis or abnormal communications between the gastrointestinal tract and the skin, with or without persistent clinical sepsis [29]. Approximately, one-third of enterocutaneous fistulae will close spontaneously with proper supportive care, control of sepsis, and nutritional support [30]. Wainstein et al. [31] reported that fistulae healed spontaneously in 46 % of patients, within a mean period of 90 days (range 8–370 days). Peng et al. [32] reported that irrigation-suction through the drainage tubes was effective in approximately 75 % of patients with leakage, without the need for surgical intervention. In their study, the median irrigation time when leakage occurred was 21 days (range 5–55 days). In the current study, the median interval between PAD puncture and complete resolution was 19 days (range 2–357 days). There are wide variations in the PAD period for postoperative intra-abdominal abscesses. The vast majority of studies on PAD for postoperative intra-abdominal abscesses have reported technical success based on short-term results, without long-term follow-up of individual patients, even though some had enteric communications [33–35]. However, long-term follow-up is necessary to accurately assess the complete resolution rate for postoperative intra-abdominal abscesses after PAD.

It has been reported that postoperative abscesses are significantly more likely than non-postoperative abscesses to be improved by PAD [36]. However, no published studies, except for that of Benoist et al., have analyzed patients who underwent PAD as the initial therapy for postoperative intra-abdominal abscesses, to find the factors predictive for success using multivariate regression analysis [33, 34, 37]. Benoist et al. examined the factors predictive of PAD failure for postoperative intra-abdominal abscesses in 73 patients and found that the absence of antibiotic therapy and an abscess diameter of <5 cm were the only two independent factors associated with failure of PAD. These authors also showed that even complex postoperative abscesses, such as those associated with enteric fistulae, were not associated with failure. The overall success rate in the current study was 85.6 % after 1 year of follow-up, which is consistent with the high success rates reported in previous studies [20, 26, 27, 37]. Multivariate analysis showed that a shorter interval between surgery and onset, and having multiple abscesses, but not the use of antibiotic therapy or the size of the abscess, were related to failure of PAD. Benoist et al. reported that patients with small abscesses in the failure group required repeat surgery for persistent or recurrent sepsis after drain removal, probably because of incomplete drainage. In our study, when abscess drainage was insufficient, the catheter was exchanged for a thicker one or it was moved to a position that allowed sufficient drainage. This adaptable drainage technique may have been an important factor in improving the outcome. Benoist et al. also reported that the absence of antibiotic therapy was an independent factor for failure of PAD. We did not give antibiotic therapy to patients with mild symptoms of an abscess; thus, the indications for antibiotic therapy may have been different in the two studies. No previous study has identified the interval

between surgery and abscess onset as a significant predictive variable for failure of PAD. However, the early onset of postoperative intra-abdominal abscesses may reflect their severity.

In this study, the success rate of PAD was 78.0 % (32/41) for patients with inflammatory bowel disease, whereas it was 90.5 % (57/63) for those without inflammatory bowel disease ($p = 0.1396$); however, inflammatory bowel disease was not related to the unsuccessful outcome statistically. Six of nine patients who underwent, or would undergo, elective surgery for an enteric fistula had inflammatory bowel disease. Moreover, the proportion of patients with inflammatory bowel disease needing elective surgery for an enteric fistula was 14.6 % (6/41), whereas the proportion of patients without inflammatory bowel disease needing elective surgery for an enteric fistula was 4.8 % (3/63) ($p = 0.1636$). All in all, the proportion of patients with inflammatory bowel disease, who needed elective surgery for an enteric fistula, was not higher statistically.

We evaluated the rate of complete resolution within the first 10 weeks, and compared the median PAD periods in Groups A and B. The rate of complete resolution of single and late-onset abscesses within the first 10 weeks after PAD was very high. All of the patients with abscesses in the failure group also had enteric fistulae, demonstrating that enteric fistula was related to the unsuccessful outcome of PAD. There was no significant correlation between the absence of enteric fistulae and single and late-onset abscess, so single and late-onset abscesses did not indicate an absence of enteric fistulae. Even if abscesses related to enteric fistula were present, the success rate of PAD for single and late-onset abscesses was very high.

Enteric fistulas during PAD were detected in 51.0 % of the patients in this study; however, the types of enteric fistula that tended to be cured by PAD were not analyzed. Campos et al. [38] and Gonzalez-Pinto et al. [39] reported that spontaneous closure was more likely for low-output fistulas, and those caused by surgery, those with free distal flow, healthy surrounding bowel, simple fistula with no associated abscess cavity, a fistula tract >2 cm, a fistula tract not epithelialized, an enteral defect <1 cm, a low fistula output, and no co-morbidity.

The potential limitations of our study include that it was a retrospective cohort series with a study population that was heterogeneous because of the wide variations in the disease and operative procedures. The decision of whether to employ PAD was at the discretion of the surgeon, which could have resulted in selection biases, and the data would be difficult to extrapolate to general patients undergoing gastrointestinal surgery. Multivariate logistic regression analysis was performed to minimize the effect of confounding factors. In addition, the effectiveness of conservative therapy such as nutritional management, the administration of octreotide and wound care, should be taken into consideration when examining factors that affect enteric fistulae closure. In this study, we focused on the relationship between patient-, surgery-, abscess- and drainage-related factors, and the outcome after PAD with long-term follow-up.

In conclusion, we evaluated the outcome of PAD in patients with intra-abdominal abscesses after recent gastrointestinal surgery. PAD is a safe and effective procedure for postoperative intra-abdominal abscess, with a high success rate and a low complication rate. We found that a single abscess and its late onset are independent predictors for a successful outcome of PAD. Conservative treatment within the first 10 weeks may be a better choice for patients with single and late-onset abscesses, even if persistent enteric fistulae are present. Initial recognition of the day of onset and the number of abscesses is important for providing prognostic information, which may subsequently influence the choice of treatment. Despite the establishment of modern strategies aimed at preventing surgical site infection, PAD remains an important factor in the postoperative management of gastrointestinal surgery in Japan. Further studies applying these prognostic models to different populations and larger numbers of patients are needed to validate and refine the models and generalize the results.

Conflict of interest Yoshiki Okita and his co-authors have no conflict of interest.

References

1. Montgomery RS, Wilson SE. Intraabdominal abscesses: image-guided diagnosis and therapy. Clin Infect Dis. 1996;23:28–36.
2. Branum GD, Tyson GS, Branum MA, Meyers WC. Hepatic abscess. Changes in etiology, diagnosis, and management. Ann Surg. 1990;212:655–62.
3. Gerzof SG, Robbins AH, Johnson WC, Birkett DH, Nabseth DC. Percutaneous catheter drainage of abdominal abscesses: a five-year experience. N Engl J Med. 1981;305:653–7.
4. vanSonnenberg E, Wittich GR, Goodacre BW, Casola G, D'Agostino HB. Percutaneous abscess drainage: update. World J Surg 2001; 25:362–9; discussion 70–2.
5. Men S, Akhan O, Koroglu M. Percutaneous drainage of abdominal abcess. Eur J Radiol. 2002;43:204–18.
6. Harisinghani MG, Gervais DA, Hahn PF, Cho CH, Jhaveri K, Varghese J, et al. CT-guided transgluteal drainage of deep pelvic abscesses: indications, technique, procedure-related complications, and clinical outcome. Radiographics. 2002;22:1353–67.
7. Golfieri R, Cappelli A. Computed tomography-guided percutaneous abscess drainage in coloproctology: review of the literature. Tech Coloproctol. 2007;11:197–208.

8. Brolin RE, Nosher JL, Leiman S, Lee WS, Greco RS. Percutaneous catheter versus open surgical drainage in the treatment of abdominal abscesses. Am Surg. 1984;50:102–8.
9. Haaga JR. Imaging intraabdominal abscesses and nonoperative drainage procedures. World J Surg. 1990;14:204–9.
10. Johnson WC, Gerzof SG, Robbins AH, Nabseth DC. Treatment of abdominal abscesses: comparative evaluation of operative drainage versus percutaneous catheter drainage guided by computed tomography or ultrasound. Ann Surg. 1981;194:510–20.
11. Malangoni MA, Shumate CR, Thomas HA, Richardson JD. Factors influencing the treatment of intra-abdominal abscesses. Am J Surg. 1990;159:167–71.
12. Muller-Wille R, Iesalnieks I, Dornia C, Ott C, Jung EM, Friedrich C, et al. Influence of percutaneous abscess drainage on severe postoperative septic complications in patients with Crohn's disease. Int J Colorectal Dis. 2011;26:769–74.
13. Inoue M, Uchida K, Otake K, Koike Y, Okugawa Y, Kobayashi M, et al. Placement of prophylactic drains after laparotomy may increase infectious complications in neonates. Pediatr Surg Int. 2011;27:975–9.
14. Robinson JO. Surgical drainage: an historical perspective. Br J Surg. 1986;73:422–6.
15. Smith SR, Connolly JC, Crane PW, Gilmore OJ. The effect of surgical drainage materials on colonic healing. Br J Surg. 1982; 69:153–5.
16. Petrowsky H, Demartines N, Rousson V, Clavien PA. Evidence-based value of prophylactic drainage in gastrointestinal surgery: a systematic review and meta-analyses. Ann Surg. 2004;240: 1074–84; discussion 84–5.
17. Gaynes RP, Culver DH, Horan TC, Edwards JR, Richards C, Tolson JS. Surgical site infection (SSI) rates in the United States, 1992–1998: the National Nosocomial Infections Surveillance System basic SSI risk index. Clin Infect Dis. 2001;33(Suppl 2): S69–77.
18. Karlson KB, Martin EC, Fankuchen EI, Schultz RW, Casarella WJ. Percutaneous abscess drainage. Surg Gynecol Obstet. 1982; 154:44–8.
19. Martin EC, Karlson KB, Fankuchen EI, Cooperman A, Casarella WJ. Percutaneous drainage of postoperative intraabdominal abscesses. AJR Am J Roentgenol. 1982;138:13–5.
20. vanSonnenberg E, Ferrucci JT Jr, Mueller PR, Wittenberg J, Simeone JF. Percutaneous drainage of abscesses and fluid collections: technique, results, and applications. Radiology 1982; 142:1–10.
21. Bernini A, Spencer MP, Wong WD, Rothenberger DA, Madoff RD. Computed tomography-guided percutaneous abscess drainage in intestinal disease: factors associated with outcome. Dis Colon Rectum. 1997;40:1009–13.
22. Goletti O, Lippolis PV, Chiarugi M, Ghiselli G, De Negri F, Conte M, et al. Percutaneous ultrasound-guided drainage of intra-abdominal abscesses. Br J Surg. 1993;80:336–9.
23. Halasz NA, van Sonnenberg E. Drainage of intraabdominal abscesses. Tactics and choices. Am J Surg. 1983;146:112–5.
24. Lambiase RE, Deyoe L, Cronan JJ, Dorfman GS. Percutaneous drainage of 335 consecutive abscesses: results of primary drainage with 1-year follow-up. Radiology. 1992;184:167–79.
25. vanSonnenberg E, Wing VW, Casola G, Coons HG, Nakamoto SK, Mueller PR, et al. Temporizing effect of percutaneous drainage of complicated abscesses in critically ill patients. AJR Am J Roentgenol. 1984;142:821–6.
26. Schuster MR, Crummy AB, Wojtowycz MM, McDermott JC. Abdominal abscesses associated with enteric fistulas: percutaneous management. J Vasc Interv Radiol. 1992;3:359–63.
27. Wittich GR. Radiologic treatment of abdominal abscesses with fistulous communications. Curr Opin Radiol. 1992;4:110–5.
28. Gerzof SG, Johnson WC, Robbins AH, Nabseth DC. Expanded criteria for percutaneous abscess drainage. Arch Surg. 1985; 120:227–32.
29. Phitayakorn R, Delaney CP, Reynolds HL, Champagne BJ, Heriot AG, Neary P, et al. Standardized algorithms for management of anastomotic leaks and related abdominal and pelvic abscesses after colorectal surgery. World J Surg. 2008;32: 1147–56.
30. Schein M. What's new in postoperative enterocutaneous fistulas? World J Surg. 2008;32:336–8.
31. Wainstein DE, Fernandez E, Gonzalez D, Chara O, Berkowski D. Treatment of high-output enterocutaneous fistulas with a vacuum-compaction device. A ten-year experience. World J Surg. 2008; 32:430–5.
32. Peng J, Lu J, Xu Y, Guan Z, Wang M, Cai G, et al. Standardized pelvic drainage of anastomotic leaks following anterior resection without diversional stomas. Am J Surg. 2010;199:753–8.
33. Benoist S, Panis Y, Pannegeon V, Soyer P, Watrin T, Boudiaf M, et al. Can failure of percutaneous drainage of postoperative abdominal abscesses be predicted? Am J Surg. 2002;184:148–53.
34. Levison MA, Zeigler D. Correlation of APACHE II score, drainage technique and outcome in postoperative intra-abdominal abscess. Surg Gynecol Obstet. 1991;172:89–94.
35. Khurrum Baig M, Hua Zhao R, Batista O, Uriburu JP, Singh JJ, Weiss EG, et al. Percutaneous postoperative intra-abdominal abscess drainage after elective colorectal surgery. Tech Coloproctol 2002;6:159–64.
36. Cinat ME, Wilson SE, Din AM. Determinants for successful percutaneous image-guided drainage of intra-abdominal abscess. Arch Surg. 2002;137:845–9.
37. Bouali K, Magotteaux P, Jadot A, Saive C, Lombard R, Weerts J, et al. Percutaneous catheter drainage of abdominal abscess after abdominal surgery. Results in 121 cases. J Belge Radiol. 1993; 76:11–4.
38. Campos AC, Andrade DF, Campos GM, Matias JE, Coelho JC. A multivariate model to determine prognostic factors in gastrointestinal fistulas. J Am Coll Surg. 1999;188:483–90.
39. Gonzalez-Pinto I, Gonzalez EM. Optimising the treatment of upper gastrointestinal fistulae. Gut 2001;49(Suppl 4):iv22–iv31.

Surg Today (2013) 43:123–129
DOI 10.1007/s00595-012-0283-9

REVIEW ARTICLE

Intravital imaging of gastrointestinal diseases in preclinical models using two-photon laser scanning microscopy

Koji Tanaka · Yuji Toiyama · Yasuhiro Inoue · Keiichi Uchida · Toshimitsu Araki · Yasuhiko Mohri · Akira Mizoguchi · Masato Kusunoki

Received: 25 January 2012 / Accepted: 9 April 2012 / Published online: 4 August 2012

Abstract Two-photon laser scanning microscopy (TPLSM), relying on two-photon excitation restricted to the focal plane, has become the gold standard in biomedical research because of its ability to produce high-resolution, higher penetrating imaging of biological materials over an extended duration without an significant photobleaching. Intravital (in vivo) imaging using TPLSM for intra-abdominal organs has long been a technical challenge because of the difficulty of achieving high-quality and higher magnification imaging with acceptable cardiac and respiratory motion artifacts. A method of intravital TPLSM was developed using an organ-stabilizing system for imaging the intra-abdominal organs of green fluorescent protein transgenic mice. This method was further refined for the time-series imaging of intra-abdominal organs in the same mouse model using intravital TPLSM. These procedures allow the observation of not only a single cell or tissue microenvironment at a higher penetrating depth for a longer period of time but also to observe the same organ of the same mouse at multiple time points in preclinical models. This report presents the general principles and properties of TPLSM for biomedical research. In addition, the methods and the usefulness of time-series intravital TPLSM imaging for preclinical gastrointestinal diseases is discussed.

Keywords Gastrointestinal disease · Intravital imaging · Two-photon laser scanning microscopy · Preclinical model

Introduction

Gastrointestinal (GI) diseases such as malignancy, inflammatory bowel disease (IBD), and strangulation are the primary targets of surgical invention.

A histopathological examination of resected specimens (surgical pathology) has provided significant insight into disease status, treatment efficacy, and patient prognosis at the cellular level. Moreover, molecular examinations (molecular biology) have increased the understanding of disease at the molecular level. Histopathological and molecular approaches have significantly advanced the understanding of the pathophysiology of GI tract diseases.

However, these worthwhile approaches separately and together do not provide clinicians with all of the needed details about disease status, treatment efficacy, and the patient's prognosis. Clinicians have added the tool of intravital (in vivo) microscopy for imaging the dynamics of cell movements and changes in subcellular structures in preclinical models. This approach permits the dynamic imaging of the organs of living animals, thus leading to an enhanced understanding of "real-time" biological processes in a variety of physiological or pathological conditions [1, 2].

Two-photon laser scanning microscopy (TPLSM) has greatly facilitated and revolutionized intravital microscopic

Electronic supplementary material The online version of this article (doi:10.1007/s00595-012-0283-9) contains supplementary material, which is available to authorized users.

K. Tanaka (✉) · Y. Toiyama · Y. Inoue · K. Uchida · T. Araki · Y. Mohri · M. Kusunoki
Department of Gastrointestinal and Pediatric Surgery, Mie University Graduate School of Medicine, 2-174 Edobashi, Tsu, Mie 514-8507, Japan
e-mail: qouji@clin.medic.mie-u.ac.jp

A. Mizoguchi
Department of Neural Regeneration and Cell Communication, Mie University Graduate School of Medicine, 2-174 Edobashi, Tsu, Mie 514-8507, Japan